



Negative/positive chemotaxis of a droplet: Dynamic response to a stimulant gas

Hiroki Sakuta, Nobuyuki Magome, Yoshihito Mori, and Kenichi Yoshikawa

Citation: [Applied Physics Letters](#) **108**, 203703 (2016); doi: 10.1063/1.4952396

View online: <http://dx.doi.org/10.1063/1.4952396>

View Table of Contents: <http://scitation.aip.org/content/aip/journal/apl/108/20?ver=pdfcov>

Published by the [AIP Publishing](#)

Articles you may be interested in

[Dynamics of oppositely charged emulsion droplets](#)

Phys. Fluids **27**, 082003 (2015); 10.1063/1.4928854

[Dynamic behaviors of liquid droplets on a gas diffusion layer surface: Hybrid lattice Boltzmann investigation](#)

J. Appl. Phys. **118**, 044902 (2015); 10.1063/1.4927422

[Dynamics and fracture of ligaments from a droplet on a vibrating surface](#)

Phys. Fluids **25**, 082106 (2013); 10.1063/1.4817542

[Dynamics of acoustic droplet vaporization in gas embolotherapy](#)

Appl. Phys. Lett. **96**, 143702 (2010); 10.1063/1.3376763

[Dynamics of droplet rebound from a weakly deformable gas-liquid interface](#)

Phys. Fluids **13**, 3526 (2001); 10.1063/1.1416189

The advertisement features a blue background with a molecular structure of spheres and connecting lines. On the left, there is a thumbnail image of an 'Applied Physics Reviews' journal cover showing a 3D grid structure. The main text 'NEW Special Topic Sections' is in large white font. Below it, 'NOW ONLINE' is in yellow, followed by 'Lithium Niobate Properties and Applications: Reviews of Emerging Trends' in white. The AIP Applied Physics Reviews logo is in the bottom right corner.

NEW Special Topic Sections

NOW ONLINE
Lithium Niobate Properties and Applications:
Reviews of Emerging Trends

AIP Applied Physics Reviews

Negative/positive chemotaxis of a droplet: Dynamic response to a stimulant gas

 Hiroki Sakuta,¹ Nobuyuki Magome,² Yoshihito Mori,³ and Kenichi Yoshikawa^{1,a)}
¹Faculty of Life and Medical Sciences, Doshisha University, Kyoto 610-0394, Japan

²Department of Chemistry, Dokkyo Medical University, Tochigi 321-0293, Japan

³Department of Chemistry, Ochanomizu University, Tokyo 112-8610, Japan

(Received 16 March 2016; accepted 10 May 2016; published online 20 May 2016)

We report here the repulsive/attractive motion of an oil droplet floating on an aqueous phase caused by the application of a stimulant gas. A cm-sized droplet of oleic acid is repelled by ammonia vapor. In contrast, a droplet of aniline on an aqueous phase moves toward hydrochloric acid as a stimulant. The mechanisms of these characteristic behaviors of oil droplets are discussed in terms of the spatial gradient of the interfacial tension caused by the stimulant gas. © 2016 Author(s). All article content, except where otherwise noted, is licensed under a Creative Commons Attribution (CC BY) license (<http://creativecommons.org/licenses/by/4.0/>). [<http://dx.doi.org/10.1063/1.4952396>]

Living organisms on Earth exhibit self-propelled motion or chemotactic behavior in response to external stimuli, where motion is driven by chemical energy under isothermal conditions. In other words, organisms can transduce information into active motion through a process in which external stimuli are recognized as being favorable or unfavorable. This phenomenon is even seen in single living cells that do not have a neural net. In contrast to these observations in living organisms, the ability of human technology to create an artificial chemical system that exhibits dynamic chemotactic behavior is still in its infancy. The spontaneous motion of self-propelled droplets has recently attracted considerable attention in relation to energy transduction by living organisms, i.e., chemo-mechanical energy transduction.^{1–8} Various kinds of droplet motion driven by a gradient in interfacial tension have been reported, as well as the propelled motion caused by diffusiophoresis.^{9,10} In a related system, an oil-water system composed of an organic phase with potassium iodide and iodine and an aqueous phase containing stearyltrimethylammonium chloride (STAC) exhibits self-agitation at the oil-water interface, accompanied by spatio-temporal non-equilibrium fluctuation of the interfacial tension.^{11–16} In addition, the motion of an oil droplet in an oil/water system has been shown to be chemosensitive.¹⁷ In measurements of the electrical potential at the oil-water interface in a similar system, the nature of the potential fluctuation and oscillation strongly depended on the chemical properties and the concentration.¹⁸ It was proposed that an oil-water system shows reactive spreading on a glass surface with recovery of the surface condition.^{19,20} The spontaneous motion of a self-propelled oil droplet moving on a glass substrate under an aqueous phase has been shown to be limited to the region of the acid-treated glass surface.^{21,22} Here, we report an artificial model system consisting of an oil droplet floating on an aqueous layer that exhibits chemotactic behavior in response to a gas stimulus.

Figure 1(a) shows the experimental system in which a droplet of oleic acid is situated on an aqueous layer with a depth of 1 cm. In this system, ammonia vapor was applied by moving a cotton swab wetted with 28% NH₃ liquid (Wako Pure Chemical Industries) close to the oil droplet. Figure 1(b) shows an example of the repulsive motion of a 25 μl oleic acid droplet in response to ammonia vapor, indicating

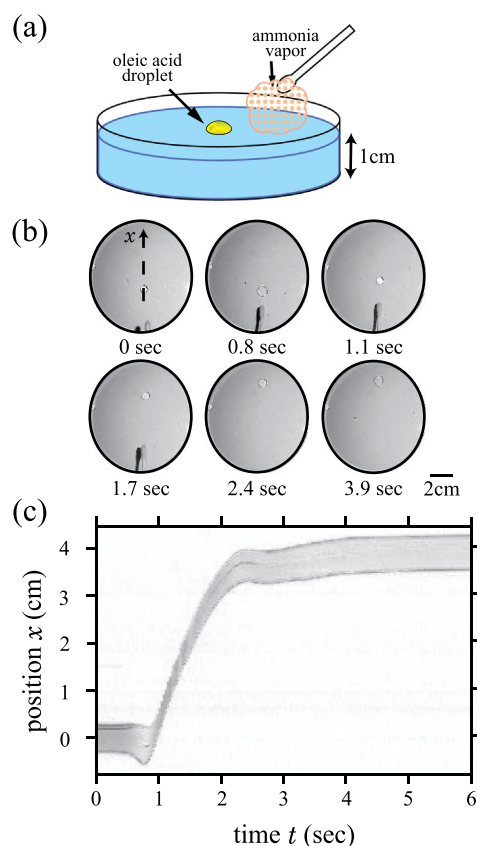


FIG. 1. Experimental observation of the negative chemotactic behavior of an oleic acid droplet floating on an aqueous solution (a) Experimental setup: ammonia vapor is applied by using a cotton swab wetted with NH₃ liquid. (b) Snapshots of an oleic acid droplet moving away from ammonia vapor. (c) Spatio-temporal diagram of droplet motion, where $x=0$ corresponds to the center of the droplet at the initial position.

^{a)}Author to whom correspondence should be addressed. Electronic mail: keyoshik@mail.doshisha.ac.jp

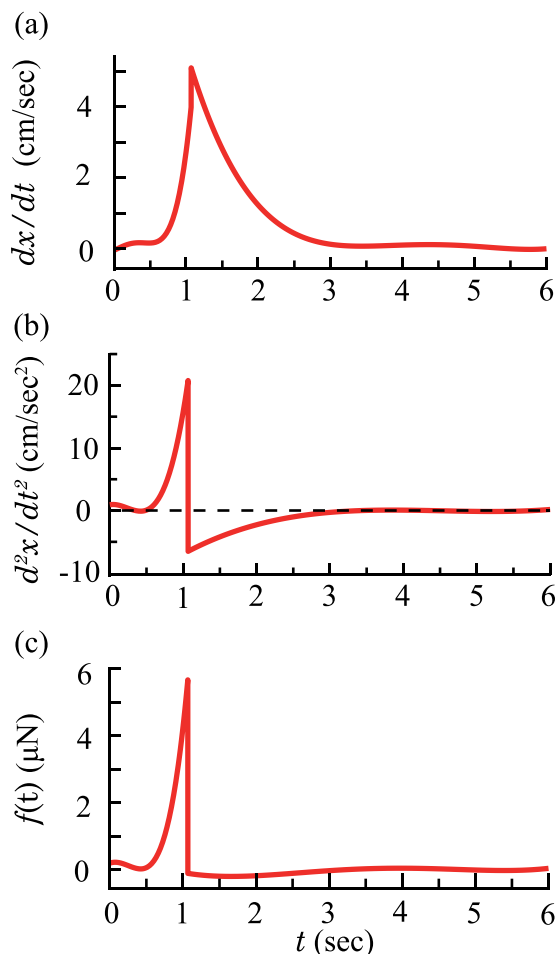


FIG. 2. Time-dependent characteristics of repulsive motion of the droplet shown in Fig. 1. (a) and (b) Profiles of the velocity and acceleration of the droplet evaluated through the time derivative and second-derivative, respectively, of the spatio-temporal diagram in Fig. 1(c). (c) Profiles of the propelling force evaluated from an analysis of the time-dependent changes in velocity and acceleration, by adapting a phenomenological kinetic equation: $m \frac{d^2x}{dt^2} + \zeta \frac{dx}{dt} + f(t) = 0$.

negative chemotaxis. To analyze the motion of the droplet in a quantitative manner, we created a spatio-temporal diagram of the droplet image, as shown in Fig. 1(c). The vertical axis shows the distance from point $x = 0$, which corresponds to the center of the original position. Careful inspection of the response of the droplet to ammonia vapor reveals that the

footprint of the droplet initially expands while it remains at the initial position for ca. 0.8 s. This increase in area implies that there is a decrease in interfacial tension at the oil-air and/or oil-water interface. The droplet then accelerates and finally stops at ca. 4 s after application of the vapor. Such repulsive motion as exemplified in Fig. 1 was confirmed to be highly reproducible. We also noted that the lag-time before the appearance of the escaping motion, e.g., ca. 1 s in Fig. 1(c), tended to increase with an increase in the distance between the floating oil droplet and the cotton swab wetted with NH_3 liquid.

We performed a time derivation of the time-dependent change in the position of the center of the droplet and obtained the time course of the droplet velocity dx/dt , as shown in Fig. 2(a). Similarly, Fig. 2(b) shows the time-dependent change in acceleration d^2x/dt^2 . We can analyze these time-dependent profiles by using the simple equation of motion in

$$m \frac{d^2x}{dt^2} + \zeta \frac{dx}{dt} + f(t) = 0, \quad (1)$$

where m [kg] is the mass of the droplet, ζ [Pa s m] is the viscosity coefficient, and $f(t)$ [N] is the driving force. We can reasonably assume that the velocity profile at the point at which acceleration switches from positive to negative is given under the condition $f(t) \approx 0$. Thus, from curve-fitting with a single exponent over the portion of the curve with a decrease in velocity ($t > 1.2$ s), we evaluated the effective viscosity ζ by using a value of $m = 22 \times 10^{-6}$ kg for 25 μl oleic acid (density: 0.89 g/cm³). With this value of ζ , we can evaluate the time-dependent change in the driving force, as shown in Fig. 2(c). In this figure, the apparent force $f(t)$ is almost null except for the period between 0.5 and 1.0 s, which supports the validity of our analysis based on the rather simple kinetic equation in Eq. (1). Note that the actual friction has two different origins: usual fluidic friction at a mesoscopic scale and molecular friction due to absorbance and desorption at the interface.²³ In a future study, it may be of interest to evaluate the origin of the apparent friction based on careful measurements.

Next, to clarify the mechanism of the stimulus-induced vectorial motion of the droplet through observation of the aqueous layer, we monitored the motion of polyethylene beads floating on the surface to visualize surface flow (see Fig. 3(a)), where the average diameter of the polyethylene

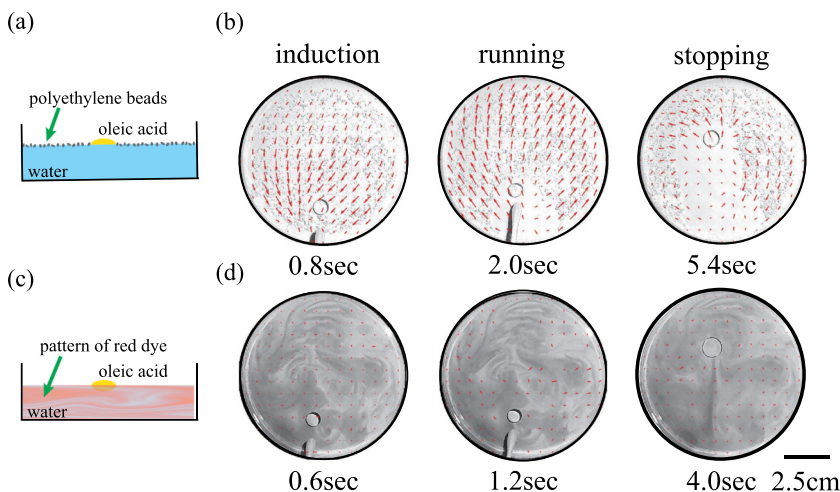


FIG. 3. Flow profiles accompanied by the generation of chemotactic behavior. (a) Schematic representation of the system for observing interfacial flow. (b) Surface flow obtained by an analysis of the velocity field with the PIV plugin for MATLAB visualized by polyethylene beads. (c) Schematic representation of the system for observing internal flow. Internal flow was visualized with the use of a hydrophilic red dye. (d) Velocity field analyzed with PIV by measuring the deformation of the diffusion pattern of the dye.

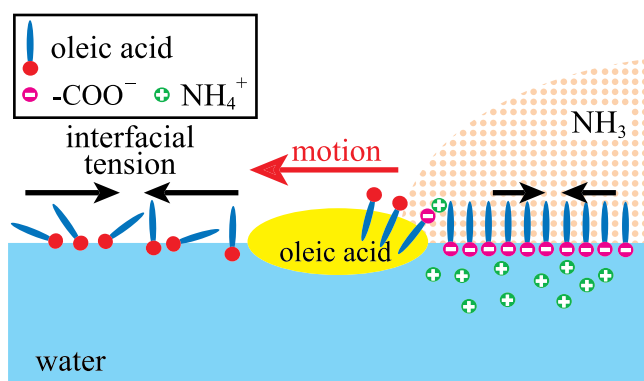


FIG. 4. Proposed mechanism of the negative chemotactic behavior of an oleic acid droplet. The gradient of interfacial tension drives the droplet away from the stimulating gas, resulting in negative chemotactic behavior.

particles is $180\ \mu\text{m}$ (CL-2507, Sumitomo Seika Chemicals Co., Ltd.). Figure 3(b) shows representative profiles of surface flow for the three stages of motion: induction stage (0.8 s), running stage (2.0 s) and stopping stage (5.4 s). The velocity field of the flow was obtained with the Particle Image Velocimetry (PIV) plugin for MATLAB. In the induction stage, the surface layer flows toward the stimulant gas. In this stage, the droplet tends to expand on the surface layer, as shown in Fig. 1. In the running stage, the direction of flow is almost opposite that in the induction stage, suggesting that the repulsive motion of the droplet coincides with the direction of flow. In the stopping stage, the directional surface flow tends to decay gradually. Figures 3(c) and 3(d) show flow profiles in the bulk aqueous solution, where the aqueous layer was prepared by the addition of small amount of $0.5\ \mu\text{M}$ of hydrophilic red dye (Ponceau 4R; trisodium (8Z)-7-oxo-8-[(4-sulfonatophthalen-1-yl)hydrazinylidene]naphthalene-1,3-disulfonate, available from Kyoritsu Foods, Inc.) to distilled water to clearly visualize the system. To visualize the internal flow of the aqueous phase, the red dye was not thoroughly mixed in the water. In contrast to the profiles regarding surface flow, there is very little motion of the liquid inside the aqueous layer. Based on these observations, the driving force of the running droplet is most likely the force acting at the interface, i.e., the gradient of the surface tension should act as the driving force for the vectorial motion of the droplet.

Figure 4 shows a schematic representation of the mechanism by which the droplet moves away from the gas

stimulus. With the application of ammonia vapor, the oleic acid located at the oil/air interface undergoes an acid-base reaction. The ionized molecules of oleic acid decrease the oil/air interfacial tension, and then cause flattening of the droplet as exemplified in the initial stage of vapor application at around 1 s. Successively, the negatively charged oleate molecules, through the binding of NH_3 to the carbonyl group, tend to spread onto the water/air interface, and this phenomenon would be more prominent on the side closer to the vapor source. Thus, the water/air interfacial tension decreases on this side. As a result, there is a large difference in interfacial tension between the sides of the droplet, and this propels the droplet to move away from the vapor source. The significant fluidic flow on the surface of the aqueous layer (Fig. 3(b)) and the stationary bulk phase (Fig. 3(d)) support the validity of this mechanism.

Figure 5 shows the attractive motion or positive chemotaxis of a $25\ \mu\text{l}$ aniline droplet floating on an aniline-saturated aqueous phase. With the application of hydrochloric acid vapor, the droplet tends to approach the vapor source. In this experiment, we consider that aniline molecules tend to form a monolayer at the water/air interface in the absence of the vapor. The contact angle of the aniline droplet is relatively small compared to that in the experiment with oleic acid, as shown in Fig. 1. In this case, the interfacial tension close to the gas stimuli is considered to increase because the positively charged aniline complexed with hydrochloric acid tends to dissolve into the bulk aqueous layer, i.e., a gradient of interfacial tension is generated between the sides of the droplet. Thus, we can explain the positive chemotaxis of the aniline droplet caused by exposure to the acidic gas.

We have described the negative and positive chemotaxis of an oil droplet floating on an aqueous phase. Negative chemotaxis is observed for a droplet with a weakly acidic molecule, i.e., oleic acid, stimulated by the relatively strong alkaline vapor of NH_3 . In contrast, positive chemotaxis is generated for the combination of a weakly alkaline oil and the strong acidic vapor of HCl . Based on these findings, we strongly suspect that negative/positive chemotaxis could be controlled by considering the acidity/basicity of the droplet and the stimulating gas, together with the hydrophobicity of the chemical components of the droplet. It would be interesting to examine this hypothesis in future studies.

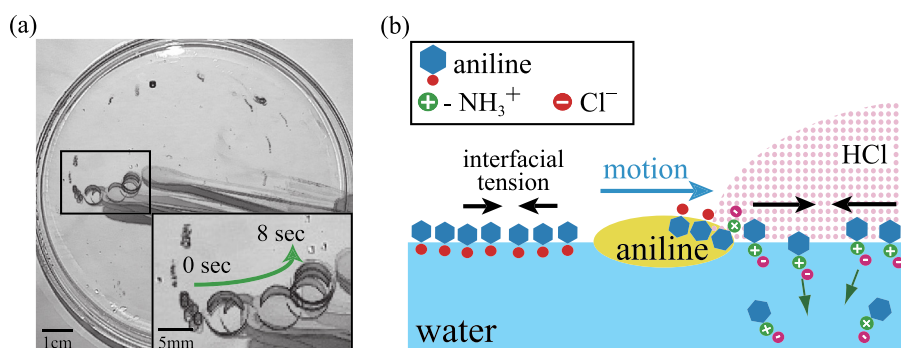


FIG. 5. Positive chemotactic behavior of an aniline droplet vs. HCl vapor. (a) Superimposed image of the aniline droplet moving toward the HCl vapor, supplied by a cotton swab wetted with hydrochloric acid solution (37%). (b) Proposed mechanism of the positive chemotactic behavior of the aniline droplet.

This work was supported by KAKENHI (15H02121, 25103012) and by the MEXT-Supported Program for the Strategic Research Foundation at Private Universities.

- ¹K. Zhang, F. Liu, A. J. Williams, X. Qu, J. J. Feng, and C.-H. Chen, *Phys. Rev. Lett.* **115**, 074502 (2015).
- ²H. Linke, B. J. Alemán, L. D. Melling, M. J. Taormina, M. J. Francis, C. C. Dow-Hygelund, V. Narayanan, R. P. Taylor, and A. Stout, *Phys. Rev. Lett.* **96**, 154502 (2006).
- ³T. Ban, T. Yamagami, H. Nakata, and Y. Okano, *Langmuir* **29**, 2554 (2013).
- ⁴L. Martiradonna, *Nat. Mater.* **14**, 463 (2015).
- ⁵F.-C. Wang, F. Yang, and Y.-P. Zhao, *Appl. Phys. Lett.* **98**, 053112 (2011).
- ⁶J. Zhang, Y. Yao, L. Sheng, and J. Liu, *Adv. Mater.* **27**, 2648 (2015).
- ⁷T. Ban and H. Nakata, *J. Phys. Chem. B* **119**, 7100 (2015).
- ⁸M. Schmitt and H. Stark, *Phys. Fluids* **28**, 012106 (2016).
- ⁹H. J. Keh and J. S. Jan, *J. Colloid Interface Sci.* **183**, 458 (1996).
- ¹⁰J. Palacci, B. Abecassis, C. Cottin-Bizonne, C. Ybert, and L. Bocquet, *Phys. Rev. Lett.* **104**, 138302 (2010).
- ¹¹M. Dupeyrat and E. Nakache, *Bioelectrochem. Bioenerg.* **5**, 134 (1978).
- ¹²E. Nakache, M. Dupeyrat, and M. Vignes-Adler, *J. Colloid Interface Sci.* **94**, 187 (1983).
- ¹³S. Kai, E. Ooishi, and M. Imasaki, *J. Phys. Soc. Jpn.* **54**, 1274 (1985).
- ¹⁴S. Kai, S. C. Muller, T. Mori, and M. Miki, *Phys. D* **50**, 412 (1991).
- ¹⁵K. Yoshikawa and N. Magome, *Bull. Chem. Soc. Jpn.* **66**, 3352 (1993).
- ¹⁶N. Magome and K. Yoshikawa, *J. Phys. Chem.* **100**, 19102 (1996).
- ¹⁷S. Nakata, K. Takemura, and Y. Hayashima, *Forma* **13**, 387 (1998).
- ¹⁸K. Yoshikawa and Y. Matsubara, *J. Am. Chem. Soc.* **106**, 4423 (1984).
- ¹⁹A. Shioi, K. Katano, and Y. Onodera, *J. Colloid Interface Sci.* **266**, 415 (2003).
- ²⁰Y. Sumino, N. Magome, T. Hamada, and K. Yoshikawa, *Phys. Rev. Lett.* **94**, 068301 (2005).
- ²¹Y. Sumino, H. Kitahata, K. Yoshikawa, M. Nagayama, S. M. Nomura, N. Magome, and Y. Mori, *Phys. Rev. E* **72**, 041603 (2005).
- ²²T. Toyota, N. Maru, M. M. Hanczyc, T. Ikegami, and T. Sugawara, *J. Am. Chem. Soc.* **131**, 5012 (2009).
- ²³Q. Yuan, X. Huang, and Y.-P. Zhao, *Phys. Fluids* **26**, 092104 (2014).